Structural Basis of the Tight Binding of Pyridoxal 5′-Phosphate to a Low Molecular Weight Protein Tyrosine Phosphatase†

Ming Zhou and Robert L. Van Etten*

Department of Chemistry, Purdue University, West Lafayette, Indiana 47907-1393

Received October 5, 1998; Revised Manuscript Received November 16, 1998

ABSTRACT: Pyridoxal 5′-phosphate (PLP) binds tightly to bovine low M_r protein tyrosine phosphatase (BPTP), but it is a very poor substrate for the enzyme. The structural basis of this tight binding of PLP is examined here by a variety of methods. Binding constants of a number of PLP analogues were measured with wild-type BPTP, and PLP binding constants of some site-specific mutants of BPTP were determined at pH 5.0 through the use of several independent methods. The tight binding of PLP (K_i = 7.6 μM) causes a downfield shift of the His-72 $C^{\epsilon 1}H$ resonance in the ^1H NMR spectrum of the protein, consistent with a structural alteration in the phosphate binding loop transmitted through a complex hydrogen bond network that exists between His-72 and Asn-15, which is a residue in the phosphate binding loop. ^1H NMR spectroscopy with an MLEV-17 spectral editing scheme was used to monitor the aldehyde resonance of PLP during titration of a catalytically inactive C12A mutant of BPTP. The aldehydic proton resonance of PLP shifted from 10.43 to 10.26 ppm upon complex formation with the C12A mutant. This resonance occurs far from the region where a hemithioacetal hydrogen would be expected to appear, consistent with the conclusion that the Cys-17 side chain of BPTP does not add to the aldehyde group of PLP. UV−visible spectrophotometric titration also supported this conclusion. The binding constant of PLP to a C17A mutant was similar to that exhibited with wild-type protein. These results show that Cys-17 makes virtually no contribution to the tight binding of PLP by BPTP, in contrast to a published report that it is "essential" for binding PLP. On the other hand, Asp-129 of BPTP was found to be very important for binding PLP. It is concluded that Asp-129 binds to the pyridinium nitrogen of PLP and that this renders Asp-129 effectively unavailable to serve its essential catalytic role as a general acid. The interactions described here should be useful in the design of specific inhibitors of this and related phosphotyrosyl protein phosphatases.

Protein phosphorylation and dephosphorylation are common and important mechanisms of cellular regulation (*1, 2*). One major group of enzymes responsible for hydrolyzing phosphotyrosyl residues off of other proteins is the protein tyrosine phosphatases (*3*). A minimal signature sequence for the phosphate binding site, CXXXXXR, is highly conserved among all the PTPases[1] (*6*). A PTPase subfamily, the low molecular weight PTPase, has been extensively investigated (*7*−*13*). The three-dimensional structure of low molecular weight PTPase from bovine heart (BPTP) has been determined independently and simultaneously by both crystallographic and NMR methods (*14*−*16*). The human enzyme structure has recently been described (*17*). These structures show that two cysteine residues, Cys-12 and Cys-17, are located in the active site region. Kinetic and ^{31}P NMR studies demonstrated that there is a covalent phosphocysteine intermediate in reactions catalyzed by this enzyme (*4*), while mutagenesis studies definitively established that Cys-12 but not Cys-17 is necessary for catalytic activity (*12*). Asp-129 was identified as the essential general acid proton donor to the leaving group in the catalysis (*18*). The high-resolution crystal structure of a transition state analogue complex has recently been presented (*19*). That study established the critical role played by enhanced hydrogen-bonding interactions that occur in the transition states for phosphorylation and dephosphorylation, relative to the ground state reactant complex.

It has been demonstrated that PLP can act as a strong competitive inhibitor of BPTP (*21*). Pyridoxal 5′-phosphate (vitamin B_6; PLP) is an essential cofactor for many decarboxylases and aminotransferases (*20*). In most such cases, the interaction between PLP and an enzyme involves the aldehyde group of the cofactor and a lysine residue of the protein. In the case of BPTP, the possible presence of a covalent interaction between PLP and a lysine residue of BPTP was discounted on the basis that reduced Schiff base intermediates were not trapped upon borohydride treatment. On the basis of a kinetic examination of a C17S mutant of BPTP fused to maltose binding protein, it was concluded that "the Cys-17 sulfur atom is essential for PLP binding" (*21*). The molecular nature of the putative interaction between Cys-17 and the aldehyde group of PLP was not identified.

† This work was supported by USDHHS Research Grant GM 27003.

* To whom correspondence should be addressed.

[1] Abbreviations: PTPase, protein tyrosine phosphatase; BPTP, bovine low molecular weight protein tyrosine phosphatase, with the sequence as described in ref *4*; PLP, pyridoxal 5′-phosphate; HCPTP-A and -B, two isoenzymes of the low molecular weight, human phosphotyrosyl protein phosphatase, with the sequences as described in ref *5*; EcAP, *Escherichia coli* acid phosphatase; DTT, DL-dithiothreitol; WT, wild type; NMR, nuclear magnetic resonance; *p*NPP, *p*-nitrophenyl phosphate.

10.1021/bi9823737 CCC: $18.00 © 1999 American Chemical Society
Published on Web 02/10/1999

The interaction of PLP with another type of phosphomonoesterase has previously been studied with care and established to involve a cysteine residue. Gao and Fonda first purified and characterized a pyridoxal phosphatase from human erythrocytes (*22, 23*). With the aid of a variety of thiol-specific chemical modification methods, they identified an essential cysteine residue in the enzyme and established that the catalytic mechanism involved a covalent phosphoenzyme intermediate (*24*). Arginine and histidine residues were also suggested to be at or near the active site and to play roles in substrate binding and/or catalysis (*25*). This was the first well-studied case that involved a cysteine residue in the interaction between PLP and a phosphatase. The information provided from that study was potentially relevant to the present case because BPTP and pyridoxal phosphatase might possess similar modes of PLP binding.

The design and synthesis of molecular inhibitors of PTPases are topics of growing significance. Many studies have focused on the structure of protein phosphatases and the physiological roles that the phosphatases may play in vivo. However, there is comparatively little information on specific inhibition of phosphatases. For example, certain phosphonic acid derivatives have been found to be potent inhibitors of PTP1B (*26*) and of CD45 (*27*). The inhibition of a specific protein tyrosyl phosphatase that negatively regulates a growth factor receptor could act to potentiate the action of endogenous growth factors. Such a rationale has been utilized in connection with the design of human prostatic acid phosphatase inhibitor (*28*). It has been suggested that the low M_r PTPase is a negative regulator of insulin-mediated mitotic signaling (*29*). Consequently, the inhibition of the low M_r PTPase could have potentiating effects on the action of insulin.

The present study examines the molecular basis of the strong binding of PLP to the low molecular weight protein tyrosine phosphatase. By testing a series of derivatives of a potent inhibitor, such as a phosphatase inhibitor, it is often possible to establish the contributions of each part of the parent inhibitor (*27*). When taken together with mutagenesis and protein structure data, the binding conformation of both the inhibitor and the active site of the protein can often be precisely constructed (*30*). The present work demonstrates that an earlier published conclusion that Cys-17 is "essential" for the strong binding of PLP to the low molecular weight bovine PTPase is incorrect (*21*). Utilizing the results of spectroscopic, kinetic, and mutagenesis experiments, the present work provides a molecular analysis of the features that do in fact contribute to this binding interaction.

EXPERIMENTAL PROCEDURES

Pyridoxal, pyridoxal 5′-phosphate, deoxypyridoxine 5′-phosphate, deoxypyridoxine, *m*-hydroxybenzoic acid, *p*-nitrophenyl phosphate (*p*NPP), and *m*-hydroxybenzoic acid were from Sigma Chemical Co., while 2-hydroxy-5-nitrobenzaldehyde, 2-hydroxy-5-nitrobenzoic acid, 3-hydroxy-4-nitrobenzaldehyde, and 4-hydroxy-3-nitrobenzaldehyde were from Aldrich Chemical Co. Deuterium oxide, deuterium chloride, and sodium deuterioxide were from Cambridge Isotope Laboratories.

Expression and Purification of Proteins. WT-BPTP as well as the C12A, C17A, and C17S mutants was expressed and purified as previously described (*4, 12*). WT-BPTP, C12A-BPTP, C17A-BPTP, and C17S-BPTP were loaded on a G-25 size exclusion column that was preequilibrated with 150 mM NaCl in H_2O solution. The protein fractions were combined and concentrated to 2 mg/mL for the spectrophotometry experiments. For the NMR experiments, C12A-BPTP was concentrated and exchanged by ultrafiltration into a solution of 100 mM NaOAc-d_3 in D_2O, pH 5.0, ionic strength 150 mM, to give a volume of 0.7 mL and a protein concentration of 10 mg/mL.

Steady-State Kinetics. K_m and V_{max} values for PLP were determined for WT-BPTP at both pH 5.0 (100 mM sodium acetate buffer, 1 mM EDTA, ionic strength 150 mM), and pH 7.5 (25 mM diethylmalonic acid buffer, ionic strength 150 mM) under 37 °C. Eight different PLP concentrations ranging from 5 to 60 μM were used. Enzyme solution (100 μL) was incubated with 900 μL of PLP solution for 1 h. The amount of phosphate released was determined by a Malachite Green inorganic phosphate assay (*31*). The K_m and V_{max} values for PLP were obtained by fitting the data to the Michaelis−Menten equation using the computer program Scientist (MicroMath).

Competitive Inhibition Constant Measurements. Inhibition constants K_i (dissociation constant of the E·I complex) were measured at 37 °C at pH 5.0, 150 mM ionic strength, in a 1 mM EDTA and 100 mM sodium acetate buffer solution. Eight substrate concentrations (0.15−2 mM *p*NPP) were used. At each substrate concentration, eight inhibitor concentrations were used for initial velocity measurements. For each initial velocity measurement, substrate stock solution (4−5 mM), inhibitor stock solution (0.1 mM), and sufficient buffer solution were mixed together to give a final volume of 500 μL. These solutions were incubated at 37 °C for 5 min, and then 20 μL of BPTP solution was added to each. The reaction was allowed to proceed at 37 °C for 4 min and was stopped by adding 500 μL of 1 N NaOH. The absorbance of the solution at 405 nm was measured using a Beckman DU-68 spectrophotometer. The initial velocities were calculated from the equation: ν_0 (unit/mg) = DF × $A_{405}/(18t)/[E]$, where DF is the dilution factor (the reaction solution was diluted by adding 500 μL of 1 N NaOH stop solution), 18 is the extinction coefficient in units of mM^{-1} cm^{-1} at 405 nm, t is the reaction time in minutes, and [E] is the enzyme concentration in the reaction mixture in units of mg/mL. Measurements of the initial velocity ν_0 were done with a series of inhibitor concentrations at each substrate concentration. Several K_i measurements were also done by measuring ν_0 for phosphate release using a Malachite Green inorganic phosphate assay (*31*).

The inhibition of WT-BPTP by PLP at pH 7.5 was measured in 25 mM diethylmalonic acid buffer at an ionic strength of 150 mM, adjusted by the addition of NaCl. A double-reciprocal plot typical of competitive inhibition was obtained (Figure 1A). A Dixon plot (*32*) was employed for more accurate determination of K_i. For each distinct substrate (*p*NPP) concentration, a plot of $1/\nu_0$ vs [I] was constructed by using a linear least squares fitting program in Quattro Pro 5.0 for Windows (Borland). This gave a family of straight lines intersecting in the second quadrant (Figure 1B). The absolute value of the projection of this intersection to the [I] axis is K_i (*32*).

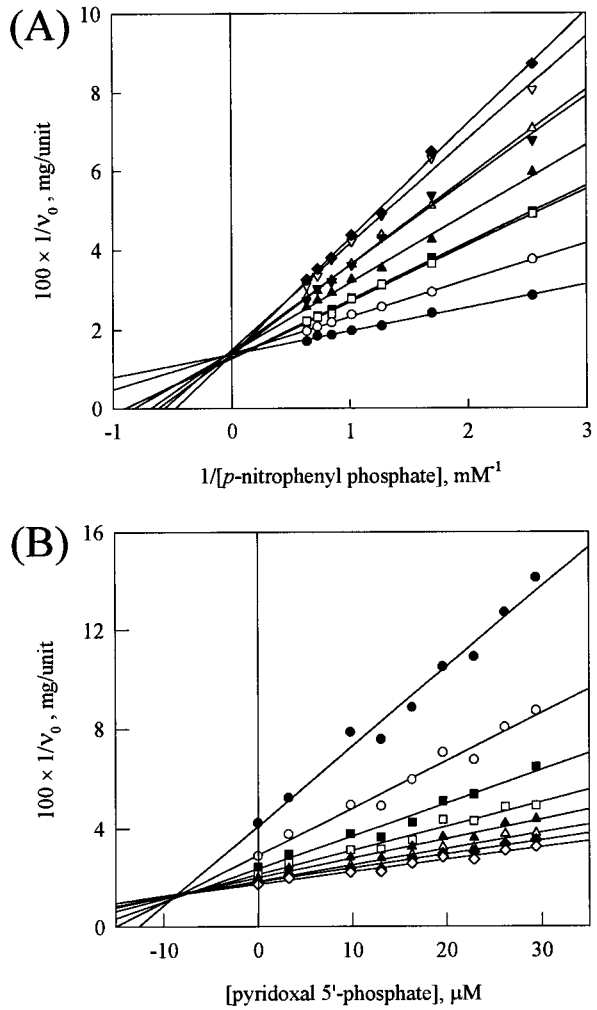

FIGURE 1: Competitive inhibition of bovine low molecular weight protein tyrosine phosphatase by pyridoxal 5′-phosphate in 100 mM sodium acetate buffer, pH 5.0, I = 150 mM. *p*-Nitrophenyl phosphate (*p*NPP) was used as the substrate. (A) Data are plotted as a double-reciprocal plot, $1/v_0$ vs 1/[S]. The pyridoxal 5′-phosphate concentrations were (●) 0 μM, (○) 3.3 μM, (■) 9.8 μM, (□) 13.1 μM, (▲) 16.3 μM, (△) 19.6 μM, (▼) 22.9 μM, (▽) 26.1 μM, and (◆) 29.4 μM. (B) Data are plotted as a Dixon plot, $1/v_0$ vs [I]. The *p*NPP concentrations were (●) 0.20 mM, (○) 0.39 mM, (■) 0.59 mM, (□) 0.78 mM, (▲) 0.98 mM, (△) 1.18 mM, (◆) 1.37 mM, and (◇) 1.57 mM.

Spectrophotometric Measurements and Inorganic Phosphate Assays. Portions of a fresh 3.6 mM PLP solution were mixed with equal volumes of 1 mg/mL WT-, C12A-, C17A-, or C17S-BPTP solution. The solutions were incubated in the dark at room temperature for 4 h. Control solutions of 1.8 mM PLP and of 0.5 mg/mL protein were treated in a similar fashion. After 4 h, 400 μL aliquots were taken from each of the solutions and used for the inorganic phosphate assay (*33*). Absorption spectra were obtained by scanning the solutions from 200 to 700 nm before and after incubation using a Hewlett-Packard 8450A UV−visible spectrophotometer. After 20 h incubation, the wavelengths of maximum absorption were determined from the spectra.

UV−Visible Spectrophotometric Titration Experiments. PLP stock solutions (1.2 mM) and C12A stock solutions (0.12 mM) in 100 mM sodium acetate buffer, pH 5.0, ionic strength 150 mM, were mixed together to give six samples. Each sample had a volume of 1.5 mL, and the C12A/PLP ratios of each sample were 0:1, 0.5:1, 1:1, 1.5:1, 2:1, and 1:0, respectively. The absorption spectra over the range from 200 to 475 nm were measured using a Hewlett-Packard 8450A UV−visible spectrophotometer.

Fluorescence Titration Measurements. The equilibrium dissociation constants K_d for ligand−BPTP complexes were measured by a fluorescence spectrophotometric method (*34*). Twelve samples with different ligand concentrations ranging from 0 to 8 × K_d were prepared in 100 mM sodium acetate buffer, pH 5.0, and 1 mM EDTA, ionic strength 150 mM, for the fluorescence intensity determination. Fluorescence intensity readings were taken immediately following the addition of BPTP to the samples. The total volume of the sample with added BPTP was kept at 500 μL. The excitation and emission wavelengths were set at 295 and 380 nm, respectively, except for C17A and D129A measurements, in which case the excitation and emission wavelengths were 280 and 380 nm, respectively. The binding constant, K_d, was calculated by nonlinear curve fitting (Scientist, MicroMath) of the data to the equations

$$F = F_0 - (F_0 - F_\infty)\frac{L}{L + K_d}$$

and

$$L = L_0 - \frac{L_0 + E_0 + K_d - \sqrt{(L_0 + E_0 + K_d)^2 - 4L_0E_0}}{2}$$

where F is the fluorescence intensity of the sample, F_0 is the fluorescence intensity at zero ligand concentration, F_∞ is the fluorescence intensity after the enzyme is completely saturated with PLP, L is the free ligand concentration of the sample, L_0 is the total concentration of PLP in each sample, and E_0 is the total enzyme concentration in each sample (*35*, *36*). All measurements were done on a Hitachi F-2000 fluorescence spectrophotometer.

^{1}H NMR Spectroscopy. The NMR samples were prepared by adding small aliquots of 15 mM PLP to 0.7 mL of a 0.8 mM C12A protein solution at a time. ^{1}H NMR spectra were obtained on a Varian Unity Plus (600 MHz ^{1}H) NMR spectrometer at 20 °C. An MLEV-17 composite-pulse sequence (90_x−spin−lock$_y$−acq) was used. Water signal suppression was achieved by placing the transmitter frequency on the residual HOD frequency and presaturating the water resonance during the relaxation delay of 1 s. Sodium 2,2-dimethyl-2-silapentane-5-sulfonate was used as an external reference at 0 ppm for all chemical shifts. Spectra with good signal-to-noise ratios were obtained at 0.6−0.8 mM protein concentration and 128−256 transients. The titration of PLP with solutions of DTT was performed in a similar fashion.

Partitioning Experiments. The initial velocity measurements were performed at 37 °C, at pH 5.0, 150 mM ionic strength, in a 1 mM EDTA and 100 mM sodium acetate buffer solution in the presence of 0−2 M methanol, using either *p*NPP or PLP as a substrate. The reaction was initiated by adding 20 μL of a catalytic concentration of the enzyme and was stopped by adding 500 μL of 1 M NaOH (500 μL of 1 M HCl was added in the case of D129E-BPTP-catalyzed PLP hydrolysis). A 4 min assay was performed with *p*NPP as a substrate, and a 120 min assay was performed with PLP as a substrate. The initial velocity was calculated from the absorbance at 405 nm and the absorbance at 380 nm for

Table 1: Spectrophotometric Changes Accompanying Phosphate Ester Hydrolysis

solution	λ_{max} (nm)[a]	extent of hydrolysis of PLP[b]
PLP	387	no detectable phosphate released
pyridoxal	<320	
C12A-BPTP + PLP	387	no detectable phosphate released
C17A-BPTP + PLP	316	0.05 mM phosphate released
C17S−BPTP + PLP	316	0.18 mM phosphate released
WT-BPTP + PLP	316	0.18 mM phosphate released

[a] Wavelength of maximum absorption (nm) at pH 5.0. [b] Following a 4 h incubation of 1.8 mM PLP without or with the indicated protein (0.5 mg/mL) at pH 5.0.

*p*NPP as a substrate and for PLP as a substrate, respectively (the absorbance at 365 nm was used in the case of D129E-BPTP-catalyzed PLP hydrolysis). The correlation of PLP concentration and the absorbance at 380 or 365 nm was predetermined under the same condition without adding the enzyme. The Michaelis−Menten parameters K_m and V_{max} were calculated by nonlinear curve fitting of the initial velocity vs substrate concentration data to the Michaelis−Menten equation (Scientist, MicroMath).

Energy Minimization Calculations. Energy minimization was done using Discover 2.9.7 with Insight II graphical molecular modeling interface software (version 95.0, Bio-Sym/MSI, San Diego). The coordinates of BPTP were taken from the refined 1.9 Å crystal structure of the BPTP−HEPES complex (*16*, *19*). The structure of pyridoxal 5′-phosphate was constructed with the Builder program of Insight II. The PLP structure was imported and docked into the active site of the BPTP structure by superimposing the phosphate group of PLP on the sulfonic group of HEPES and then deleting the HEPES molecule from the structure of the complex. A similar procedure was employed to obtain BPTP−PLP complexes having three different initial binding orientations of PLP. Mutant protein BPTP−PLP complexes were constructed using the Biopolymer module of Insight II. Each initial complex structure was subjected to 50 steps of steepest descent energy minimization and then 5000 steps of conjugate gradient energy minimization or until the convergence criterion (defined as energy derivative less than 0.001 kcal mol^{-1} $Å^{-1}$) was reached. For the energy minimization calculations, the consistent valence force field (CVFF) was used, the dielectric constant was set at 5.0, the nonbond distance cutoff was set to 20 Å, the pH was set to 5.0, and the hydrogen bond cutoff angle was set to 120°. The other parameters were set as default values.

RESULTS

PLP as a Substrate of Wild-Type and Mutant BPTP. The hydrolysis of the phosphate group of PLP is known to result in a dramatic shift in the UV absorption spectrum (*37*). This property was used in an initial assessment of the extent of hydrolysis of PLP upon incubation with BPTP or with its mutants. Extended incubation of PLP with the respective proteins showed that WT-, C17A-, and C17S-BPTP were eventually able to hydrolyze the phosphate group from PLP (Table 1). Steady-state kinetic measurement confirmed that PLP is a very poor substrate for WT-BPTP, with k_{cat} values of 0.0015 and 0.00072 s^{-1} at pH 5.0 and 7.5, respectively. These values may be compared to the k_{cat} values for *p*NPP, which are 30 and 20 s^{-1}, respectively (Table 2). Although the hydrolysis rate is very slow at low enzyme and PLP concentrations, the extent of hydrolysis becomes of practical significance at high concentrations of enzyme and PLP (such as those used for NMR measurements). Because of the catalytic inactivity of the C12A mutant (*12*), it does not significantly hydrolyze PLP even over an extended time period (Table 1). The absorption spectra accompanying the titration of C12A-BPTP with PLP are shown in Figure 2. The λ_{max} increases from 387 to approximately 415 nm. Such an increase is not consistent with covalent addition to the carbonyl of PLP (*38*, *39*).

Table 2: Michaelis−Menten Parameters for the Hydrolysis of Pyridoxal 5′-Phosphate Catalyzed by WT-BPTP[a]

pH	K_m (μM)	V_{max} (unit/mg)	k_{cat} (s^{-1})
5.0	17 ± 4	0.0049 ± 0.0005	0.0015 ± 0.0002
7.5	25 ± 11	0.0024 ± 0.0005	0.00072 ± 0.00017

[a] Measurements were made at 37 °C.

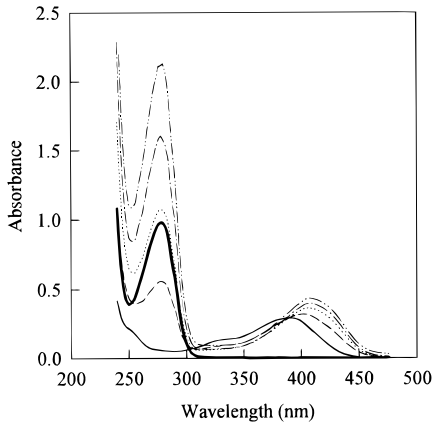

FIGURE 2: Ultraviolet−visible spectrophotometric titration of a catalytically inactive C12A mutant of BPTP with PLP. Curves: (—) 0.05 mM PLP, 0 mM C12A; (**—**) 0 mM PLP, 0.05 mM C12A; (- - -) 0.05 mM PLP, 0.025 mM C12A; (···) 0.05 mM PLP, 0.05 mM C12A; (— · —) 0.05 mM PLP, 0.075 mM C12A; (— ·· —) 0.05 mM PLP, 0.1 mM C12A.

Inhibition of WT-BPTP by PLP and PLP Analogues. Because of the large difference in the rate of hydrolysis of PLP compared to that of a good substrate such as *p*NPP, it was readily possible to measure the K_i values for PLP by treating it as an inhibitor of the hydrolysis of *p*NPP. The inhibition was carefully established to be competitive under the assay conditions used for these measurements (Figure 1). Inhibition constants for PLP and for several structural analogues are listed in Table 3. All of the inhibition patterns were competitive. Although quite different assay methods were used to measure the K_m and K_i constants (Malachite Green inorganic phosphate assay and competitive inhibition of *p*NPP, respectively), the K_m (17 μM) and K_i values (7.6 μM) for PLP with WT-BPTP at pH 5.0 are in good agreement.

^{1}H NMR Titration Analyses. The aldehydic proton of PLP can be easily identified because it resonates at a high ^{1}H NMR frequency relative to the other signals in the spectrum. Covalent and noncovalent interactions that involve the carbonyl group of PLP may generally be expected to cause the ^{1}H resonance to shift away from its original position. Consequently, ^{1}H NMR is a very sensitive tool to investigate the interaction between the enzyme and the aldehyde moiety

Table 3: Inhibition Constants of Pyridoxal 5′-Phosphate and Related Derivatives with WT-BPTP, Measured by Competitive Inhibition of the Hydrolysis of *p*-Nitrophenyl Phosphate at pH 5.0

competitive inhibitor	K_i (mM)
pyridoxal 5′-phosphate	0.0076 ± 0.0018
pyridoxal	4.6 ± 0.6
deoxypyridoxine 5′-phosphate	2.0 ± 0.4
deoxypyridoxine	1.4 ± 0.3
2-hydroxy-5-nitrobenzaldehyde	0.40 ± 0.05[a]
2-hydroxy-5-nitrobenzoic acid	1.3 ± 0.3[a]
3-hydroxy-4-nitrobenzaldehyde	1.4 ± 0.2[a]
4-hydroxy-3-nitrobenzaldehyde	1.5 ± 0.3[a]
m-hydroxybenzoic acid	5.0 ± 0.5

[a] Measured by a Malachite Green phosphate assay.

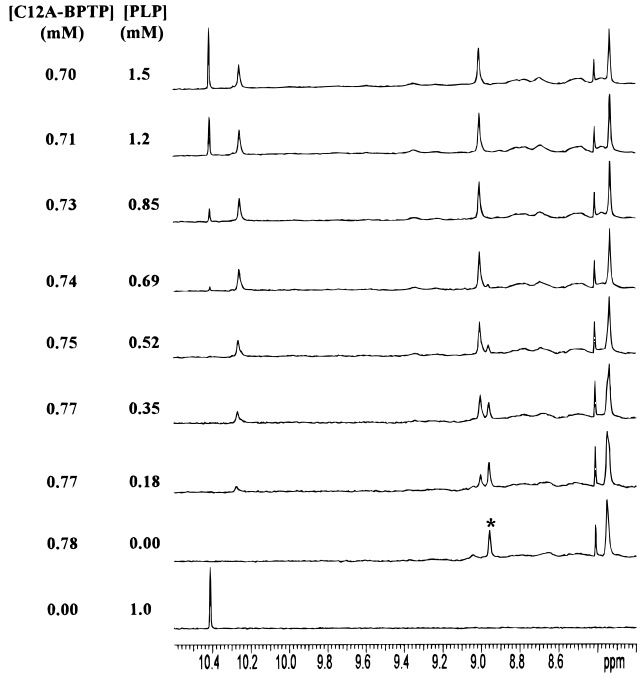

FIGURE 3: ^{1}H NMR spectrum of C12A-BPTP titrated with PLP. The aldehydic proton resonance of PLP is shifted from 10.43 to 10.26 ppm at the beginning of the titration. The 10.43 ppm resonance only reappears when an approximately stoichiometric amount of PLP has been added to the solution containing C12A-BPTP. During the titration, the His-72 C$^{\epsilon 1}$H resonance of C12A-BPTP is shifted from 8.96 to 9.00 ppm. The exchange of PLP is slow relative to the NMR time scale. The dissociation constant of the PLP−BPTP complex can be estimated to be approximately 4 μM from the line width and integral of the His-72 C$^{\epsilon 1}$H resonances.

of PLP. At the same time, resonances such as the histidine C$^{\epsilon 1}$H resonance of BPTP can also be studied to assess possible changes in the protein that may occur upon binding of PLP. Because the amide protons are highly overlapped with the histidine C$^{\epsilon 1}$H resonance, an MLEV-17 spectral editing scheme (*12*, *13*, *40*) was utilized to eliminate the amide proton resonances, which have extremely short transverse magnetization relaxation times. Due to the difference in relaxation times, the resonances of protons bonded to carbon are preserved at the end of the MLEV-17 scheme while most of the resonances of protons bonded to nitrogen are filtered out. A solution of the catalytically inactive C12A mutant of BPTP was titrated with PLP (Figure 3). In the PLP/D_2O sample spectrum, the ^{1}H NMR resonance peak at 10.43 ppm was assigned to the aldehydic proton resonance of PLP. Upon titration of PLP with the C12A mutant, this

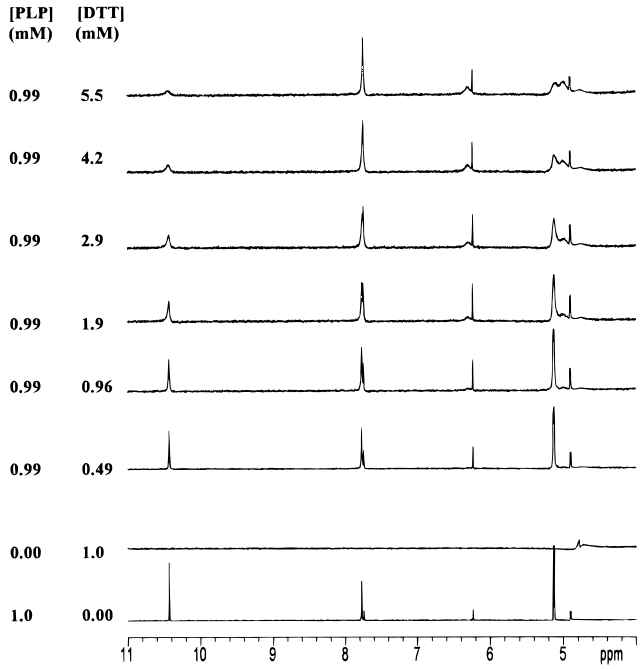

FIGURE 4: ^{1}H NMR spectrum of PLP titrated with DTT. The intensity of the aldehydic proton resonance of PLP decreases as the concentration of DTT increases. A broad peak appears at 5.0 ppm.

resonance progressively diminished in intensity until the ratio of C12A to PLP was nearly 1:1. Simultaneously, a resonance peak appeared nearby at 10.26 ppm, and its intensity increased as the titration proceeded. This new resonance peak was noticeably broader than the aldehydic peak of PLP in free solution. Also in step with these changes, the protein's His-72 C$^{\epsilon 1}$H resonance at 8.96 ppm shifted to a higher resonance frequency. Because the His-72 C$^{\epsilon 1}$H resonances of free enzyme and PLP-bound enzyme were very well resolved (Figure 3), the two forms of enzyme are under slow exchange relative to NMR time scale. If it is assumed that the rate constant for binding of PLP to BPTP is near the diffusion-controlled rate limit, then the dissociation constant of the PLP−BPTP complex can be estimated to be 4 μM, based on the line width and integrals of the His-72 C$^{\epsilon 1}$H resonances (*41*). This value is in good agreement with the K_i value (7.6 μM) determined by kinetic inhibition methods.

As a control experiment to confirm the expected effect of thiol addition to the carbonyl of PLP, a sample of PLP was titrated with excess DTT. Figure 4 shows that the intensity of the aldehyde proton resonance of PLP decreased as the concentration of DTT increased. At the same time, a broad new peak appeared at 5.0 ppm, consistent with the formation of a tetrahedral addition product and the loss of the original aldehyde functional group.

Comparison of PLP Binding by WT and Mutants of BPTP. The PLP dissociation constants measured by competitive inhibition techniques for WT-BPTP and several mutants of BPTP are listed in Table 4. The K_i for the PLP complex of C17A-BPTP is increased by less than a factor of 3 compared to the complex with WT-BPTP. In contrast, when the catalytically essential Asp-129 residue (*18*) is mutated to glutamic acid, the K_i for PLP increased by a factor of 53.

Fluorescence Measurements. Crystallographic studies had earlier revealed a tryptophan residue, Trp-49, on the protein

Table 4: Inhibition of WT-BPTP and BPTP Mutants by Pyridoxal 5′-Phosphate, Measured by Competitive Inhibition of the Hydrolysis of *p*-Nitrophenyl Phosphate

protein	K_i (mM) at pH 5.0
WT-BPTP	0.0076 ± 0.0018
	0.044 ± 0.006 (at pH 7.5)
C17A-BPTP	0.025 ± 0.003
C17S-BPTP	0.15 ± 0.02
Y131A-BPTP	0.016 ± 0.003
D129E-BPTP	0.40 ± 0.10[a]
N50A-BPTP	0.0059 ± 0.0019
W49F-BPTP	0.0189 ± 0.0046

[a] Measured by a Malachite Green phosphate assay.

Table 5: Dissociation Constants Measured by Fluorescence Perturbation at pH 5.0

enzyme−ligand complex	K_d (mM)
C17A−PLP	0.0107 ± 0.0008[a]
C12A−PLP	0.00057 ± 0.00015[c] (pH 5.0)
	0.0015 ± 0.0003[c] (pH 4.0)
D129A−PLP	0.28 ± 0.02[a]
D129E−PLP	0.48 ± 0.13[c] (pH 5.0)
	0.43 ± 0.12[c] (pH 7.5)
C12A-D129A−PLP	2.4 ± 0.02[c]
WT-BPTP−deoxypyridoxine 5′-phosphate	2.1 ± 0.5[b]
WT-BPTP−pyridoxal	0.25 ± 0.02[b]
WT-BPTP−pyridoxal + 5 mM P_i	0.28 ± 0.04[b]
WT-BPTP−PLP	0.0050 ± 0.0005[c]
WT-BPTP−PLP + 5 mM P_i	0.0161 ± 0.0013[c]

[a] Excitation at 280 nm and emission at 380 nm. [b] Excitation at 295 nm and emission at 320 nm. [c] Excitation at 295 nm and emission at 380 nm.

surface at the entrance to the active site cleft; the fluorescence properties of this tryptophan of BPTP have been intensively characterized (*16*, *34*). Because Trp-49 is near the active site, it can serve as a reporter group for changes around the active site. Ligand binding constants can be determined if the ligand molecule quenches the fluorescence exhibited by Trp-49. The emission spectrum of WT-BPTP is centered in the range from 300 to 400 nm and occurs with a reasonable quantum yield. PLP, pyridoxal, and several of their derivatives all have a strong absorption band in this wavelength region. Thus, it is possible to use the fluorescence method to determine the binding constants for these molecules. Binding constant measurements obtained by fluorescence perturbation techniques are listed in Table 5. The fluorescence K_d value of the C17A-PLP complex (10.7 μM) is in reasonable agreement with the K_i value from kinetic measurements (25 μM). However, the fluorescence K_d value for the pyridoxal complex of WT-BPTP (0.25 mM) is substantially smaller than the K_i value from kinetic measurements (4.6 mM). Significantly, the simultaneous presence of inorganic phosphate has virtually no effect on the value of K_d for pyridoxal, indicating that pyridoxal and inorganic phosphate do not bind to overlapping regions of the protein. In contrast, inorganic phosphate directly competes with the binding of PLP (Table 5).

Partitioning Experiments. The differing effects of methanol on the hydrolysis of *p*NPP and PLP as catalyzed by WT- and D129E-BPTP are illustrated in Figure 5. Consistent with earlier results, the hydrolysis rate of *p*NPP catalyzed by WT-BPTP was increased by the presence of methanol (*11*). In contrast, methanol had no effect on the hydrolysis of PLP catalyzed by WT-BPTP. For the reactions catalyzed by the D129E-BPTP mutant, methanol increased the reaction rates of both *p*NPP and PLP (Figure 5B).

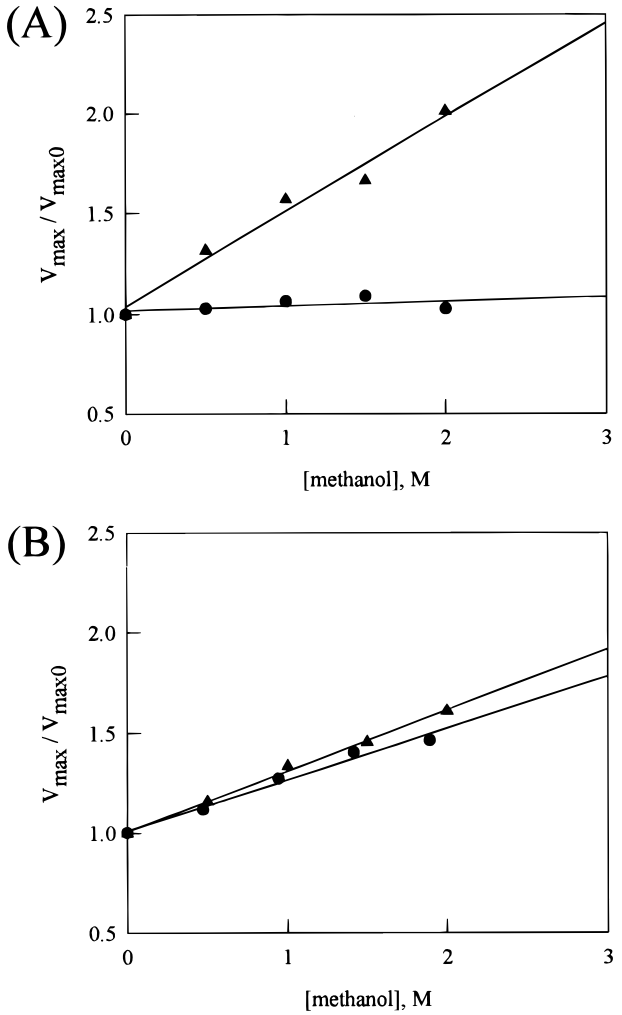

FIGURE 5: (A) Differing effects of methanol on the hydrolysis of *p*NPP (▲) and PLP (●) as catalyzed by WT-BPTP. (B) Effect of methanol on the hydrolysis of *p*NPP (▲) and PLP (●) as catalyzed by the mutant D129E-BPTP. Measurements were made at pH 5.0, in a buffer of 100 mM NaOAc, I = 150 mM, and 1 mM EDTA.

DISCUSSION

The K_m values for PLP as a substrate and the K_i for PLP measured as a competitive inhibitor of WT-BPTP are very similar. The agreement indicates that, as a substrate, the dissociation of PLP from the enzyme is rapid relative to the rate of its conversion to products. V_{max} values at representative pH values for PLP as a substrate are also very low compared to the respective values for *p*NPP.

Earlier spectrophotometric studies of PLP established that, upon hydrolysis of PLP to pyridoxal, a maximum absorption wavelength shift occurs due to the fact that the aldehyde group of PLP (387 nm) was changed to a hydrate form in pyridoxal (316 nm) (*37*). That is, the carbonyl group of pyridoxal (without the phosphate group) is more readily hydrated than is that of PLP. In fact, nearly 80% of PLP is present as the aldehyde form, whereas 98% of pyridoxal is in the hydrated form at pH 5.0 (*37*). The present UV−visible spectrophotometric studies revealed that, upon extended incubation of PLP with WT-BPTP, the wavelength of maximum absorption shifted from 387 to 316 nm, consistent

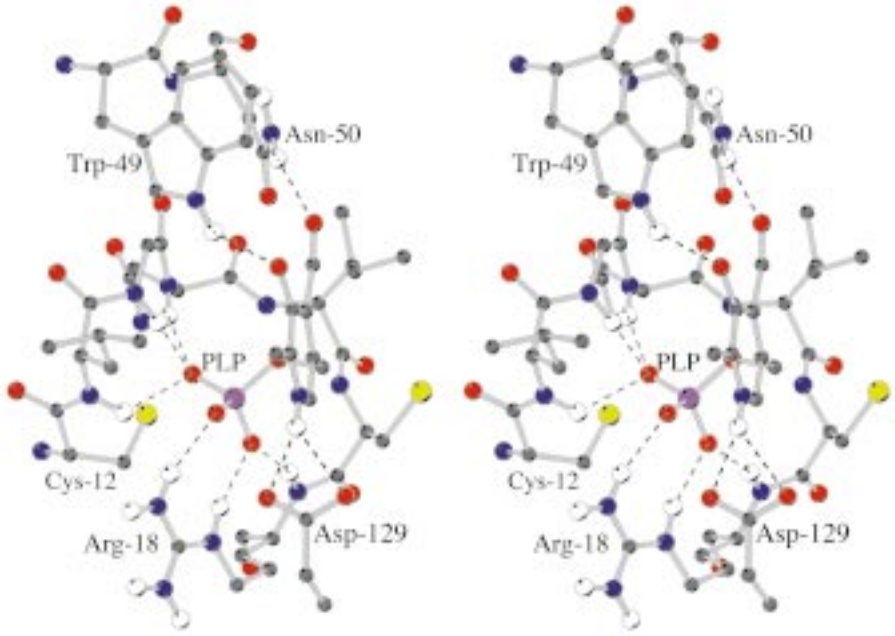

FIGURE 6: Stereo diagram of one model of the binding of PLP by BPTP. The model was generated by energy minimization calculation using Insight-Discover software (see text), and the figure was drawn with Molscript. The hydrogen bonds are shown in dotted lines.

with the hydrolysis of the phosphate group and subsequent hydration of the aldehyde in free pyridoxal. Measurement of the kinetic parameters K_m and V_{max} for PLP as a substrate of WT-BPTP confirmed this conclusion (Table 1). Although the relative enzyme activity with PLP was very low, the turnover rate was experimentally significant at the very high protein concentrations (0.5−1 mM) that were used for NMR samples. Therefore, WT-BPTP and its active mutants could not be used in spectral titration experiments. Because the C12A mutant lacks the essential nucleophilic thiolate (*12*), it has no significant activity toward pNPP or PLP. For this reason, UV−visible spectrophotometric, fluorescence perturbation, and NMR titration experiments could be performed with C12A BPTP (Figures 2 and 3; Table 5).

Quantitative fluorescence titration measurements showed that PLP binds tightly to the C12A mutant protein (Table 5). Indeed, at pH 5, the dissociation constant of the PLP-C12A complex is even smaller (0.57 μM) than the corresponding value for the PLP complex of WT protein (5.0 μM). We have previously shown that the acidity of Cys-12 is sharply perturbed in this enzyme, leading to a pK_a somewhat below 4 in the free enzyme (*42*). Elimination of the thiolate anion in the C12A mutant results in the loss of an unfavorable electrostatic interaction involving the anionic phosphate of PLP. Thus, in the C12A mutant, binding of an anionic phosphate derivative is even more strongly dominated by the combined effects of the catalytically critical backbone N−H's (*19*), the Arg-18 side chain, and the positive end of the helix dipole.

Role of Cys-17. The inhibition results show clearly that the Cys-17 residue is not important, much less essential to the binding of PLP (Table 4). The K_i measured with the C17A mutant (25 μM) is similar to that for WT-BPTP (7.6 μM). The replacement of Cys-17 by serine results in a larger K_i (150 μM), probably reflecting the greater tendency of the serine hydroxyl group to be involved in hydrogen bond interactions. The increase in K_i may be due to the presence of hydrogen-bonded water that obstructs the active site, or perhaps the serine side chain directly hydrogen bonds to neighboring protein sites and causes modest structural alterations. Even so, the C17S mutant still binds PLP more strongly than it binds the classical competitive inhibitor phosphate ion (K_i = 2.0 mM), and the C17A mutant binds PLP almost as strongly as does WT enzyme. The results of dissociation constant measurements by fluorescence (Table 5) and competitive inhibition kinetic methods (Tables 3 and 4) are in very good agreement for both the C17A-PLP and WT-BPTP−pyridoxine phosphate cases. The favorable fluorescence K_d and kinetic K_i results for the C17A-PLP complex further confirm that Cys-17 is not important for the binding of PLP. The present results are very different from those reported elsewhere (*21*), where it was claimed that the C17S mutant did not bind PLP at all and that "the Cys-17 sulfur atom was essential for PLP binding".[2]

Role of the Phosphate Group of PLP. The phosphate moiety of PLP was important for binding to BPTP. Several hydroxynitrobenzaldehyde derivatives that lacked the pyridine nitrogen and phosphate moieties caused only limited inhibition (Table 3). Given the extent of hydrogen-bonding interactions between the protein P-loop and phosphate groups of the substrate and in the transition state (*16, 19, 42*), it is not surprising that the phosphate group of PLP can be regarded as an anchor that directs the PLP to the active site. Removal of the phosphate portion of the ligand has major effects on the strength and location of binding, causing K_i to increase from 7.6 μM to 4.6 mM (Table 3). Moreover, in the case of pyridoxal (but not PLP), the fluorescence K_d (0.25 mM) is significantly smaller than the kinetic K_i (4.6 mM). Nonetheless, the kinetic measurements indicate that pyridoxal is a well-behaved competitive inhibitor of WT-BPTP. This

[2] Their results may have been in error because they were obtained with a fusion protein in which BPTP was attached to a 42 kDa maltose-binding protein. We have pointed out other erroneous results obtained with such a fusion protein (*12*).

difference means that although pyridoxal can bind relatively strongly to a region of WT-BPTP that is sensitive to fluorescence quenching, this mode of binding does not necessarily result in significant inhibition of the enzyme. To test if the binding interaction measured by fluorescence perturbation was influenced by additional small competitive inhibitors, the effect of a simultaneous presence of inorganic phosphate was measured. In the presence of 5 mM inorganic phosphate (a concentration that is 2.5 times the K_i for inorganic phosphate), the fluorescence K_d of pyridoxal changed by less than a factor of 2 (Table 5). It is likely that the binding interaction measured by fluorescence perturbation of Trp-49 involves a hydrophobic and/or stacking association of pyridoxal with the aromatic residues including Trp-49 located near the entrance to the active site (*16*). The affinity of the enzyme toward a second pyridoxal molecule is much weaker, but it is this further association that is accompanied by competitive inhibition.

Role of the Aldehydic Group of PLP. The aldehyde group of PLP was important for strong binding. When the aldehyde functionality of PLP is replaced by the methyl group in deoxypyridoxine 5′-phosphate, the dissociation constant of the complex with WT-BPTP is increased from 7.6 μM to 2.0 mM (Table 3). Energy minimization calculations were utilized to examine factors that contribute to the importance of the aldehydic oxygen of PLP to the overall binding interaction. The aldehyde function affects the electronic distribution in the pyridinium ring. In addition, the aldehydic oxygen can also form hydrogen bond(s) with nearby residues at the active site. Energy minimization calculations suggested the possible presence of hydrogen bonds between the carbonyl oxygen of PLP and the proton on the amide nitrogen of Asn-50 side chain, between the phenolic oxygen of PLP and the proton on the indole nitrogen of Trp-49, and between the phosphate group of PLP and the amide protons of the phosphate binding loop and the guanidium group of Arg-18 (Figure 6). The dissociation constants of PLP with N50A-BPTP (5.9 μM) and W49A-BPTP (18.9 μM) were very similar to the dissociation constant with WT-BPTP (7.6 μM). Although single point mutations at either Asp-50 or Trp-49 did not significantly affect the binding constant of PLP, these residues are located on a flexible loop (*14, 16*). Mutating only one residue may not be able to eliminate the hydrogen bond interaction between a specific group of PLP and BPTP.

The NMR titration results of C12A and PLP show that the aldehydic proton resonance of PLP only shifted from 10.43 to 10.26 ppm when PLP was added to the enzyme solution. This result indicates that the aldehyde group of PLP remains intact and is only participating in noncovalent interactions with surrounding groups, because any covalent interaction with the aldehyde group would be expected to cause a dramatic chemical shift change of the aldehydic proton resonance. The possibility of a covalent interaction between the aldehyde group of PLP and Cys-17 was ruled out by comparison with the DTT−PLP NMR titration results. Upon titration with DTT, the PLP aldehydic proton resonance at 10.26 ppm was replaced by a resonance at ~5.0 ppm. This change in chemical shift indicates that DTT covalently interacts with PLP via hemithioacetal formation. Earlier reports on similar types of hemithioacetal reactions investigated by NMR spectroscopy in the studies of inhibition of

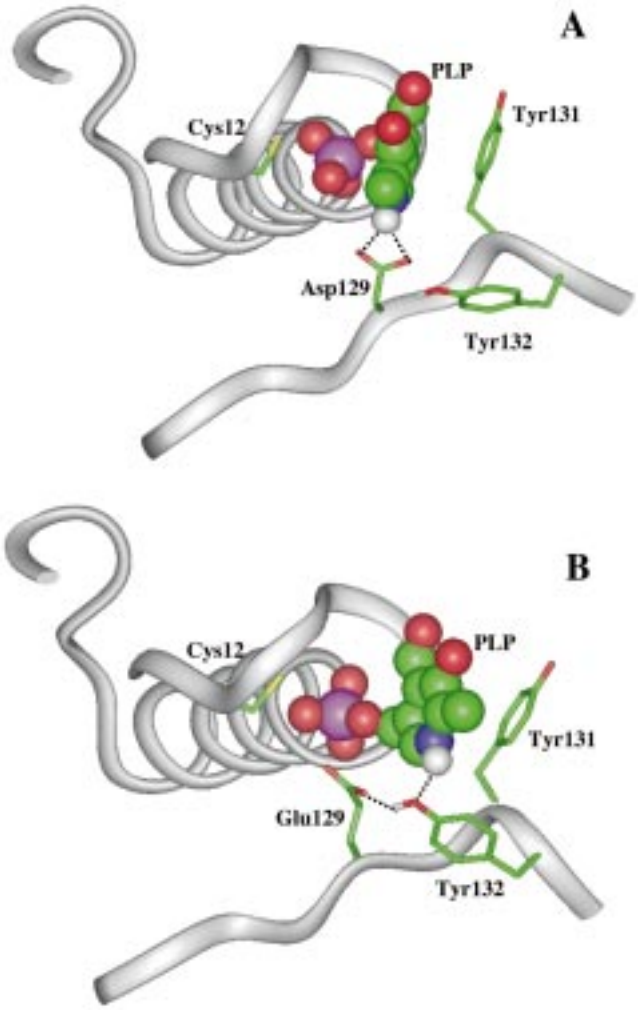

FIGURE 7: Diagrams of the WT-BPTP−PLP complex (A) and of the D129E-BPTP−PLP complex (B) after the energy minimization. The figures were drawn with Insight 97.0.

papain and papain-related model studies further support the above conclusion (*43, 44*).

Additional evidence for a noncovalent interaction was obtained by UV−visible spectrophotometric titration experiments. In pH 5.0 solution, PLP is represented by a resonance hybrid of structures a and b (*37, 45*). Hydrogen bonding of

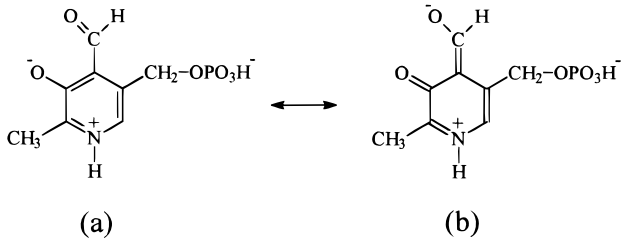

the aldehyde oxygen with solvent water is expected to further polarize the oxygen and stabilize resonance structure b. The UV−visible spectra showed that the absorption band of PLP shifted to higher wavelength when PLP binds to the C12A. This red shift may be caused by hydrogen bonding between the aldehydic oxygen of PLP and the active site of C12A, thus further stabilizing resonance structure b.

The broadened peak at 10.26 ppm is caused by the association of PLP with the relatively large enzyme molecule.

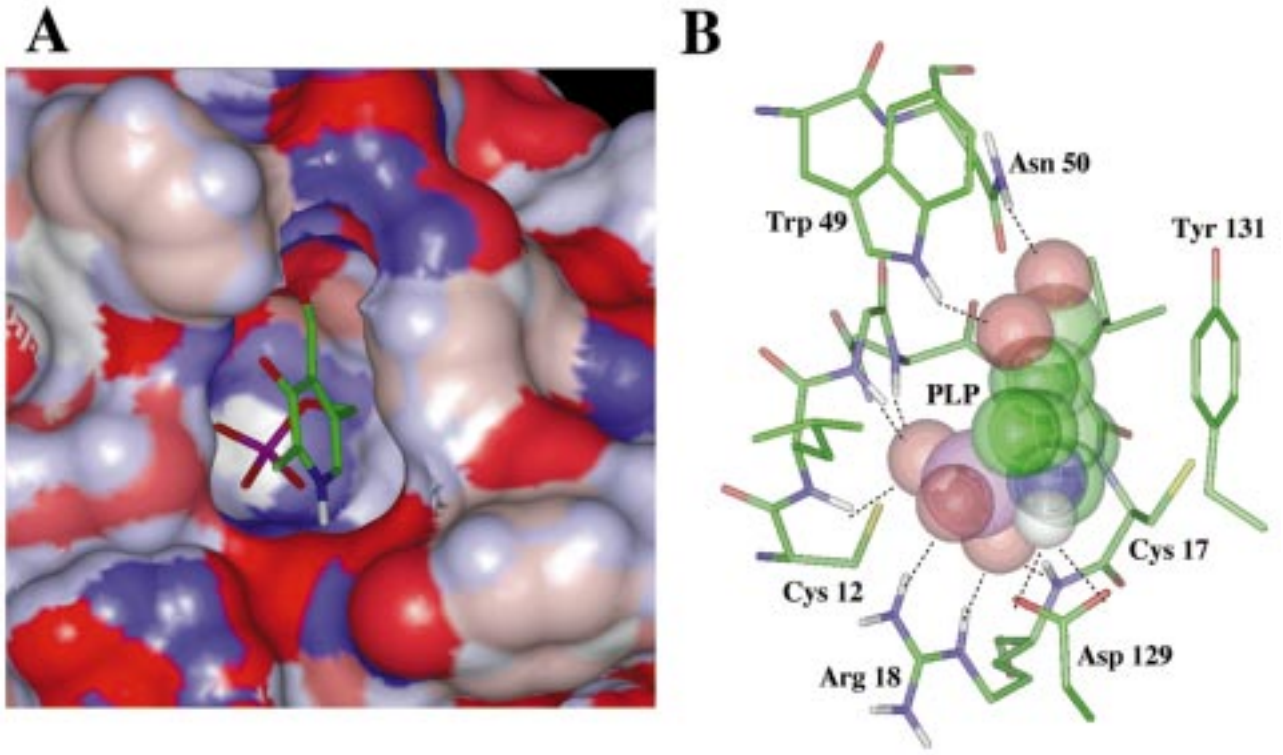

FIGURE 8: Positioning of PLP in the active site of BPTP. (A) Electrostatic surface diagram of the active site of the WT-BPTP−PLP complex generated from the energy minimization calculation with Discover 2.9. The red surface indicates the negative charges and the blue color indicates the positive charges. The PLP molecule is shown as a stick model. The diagram was drawn with Insight 97.0. (B) Stick model diagram of the active site of the WT-BPTP−PLP complex. The detailed hydrogen bond interactions are shown in dotted lines.

The binding of PLP also appears to cause a modest structural perturbation in the region of the active site, in view of the fact that the His-72 $C^{\epsilon 1}H$ resonance is shifted from 8.96 to 9.00 ppm (Figure 3). The exchange rate between free and bound PLP is relatively slow on the NMR time scale since the His-72 $C^{\epsilon 1}H$ resonance shift is clearly resolved in the spectra. From the line width and the peak integrals of the spectrum, the binding constant K_i of PLP to C12A can be estimated to be 4 μM.

Role of Tyr-131. The K_i of the PLP-Y131A complex is 16 μM, which is almost the same as that for the WT-BPTP case ($K_i = 7.6$ μM). Evidently, Tyr-131 contributes little to the binding of PLP by hydrophobic stacking interactions. However, such interactions might be important with other less polar ligands.

Role of the Pyridinium Ring of PLP. The position of the ring oxygen was important to the binding. Only 2-hydroxy-5-nitrobenzaldehyde showed some inhibition among several hydroxynitrobenzaldehydes analogues that were tested. The hydroxyl group at position 2 on the pyridine ring of PLP makes an important contribution to binding, probably by virtue of its effect on the basicity of the pyridinium ring. The pK_a of the pyridinium nitrogen of PLP is 8.33 (*37*) so the nitrogen is effectively fully protonated below pH 7.5. The negatively charged Asp-129 is probably involved in interacting with the pyridinium nitrogen via an electrostatic and/or hydrogen-bonding interaction (vide infra). The K_i of PLP with BPTP is comparable at pH 7.5 and 5.0, so a pH change of 2.5 units did not appear to alter the interaction by affecting the charge on either Asp-129 or the pyridinium nitrogen (Table 4). The phosphate group of PLP is still bound to the phosphate binding loop at the active site, while the aldehydic oxygen and exocyclic oxygen seem to interact with the residues close to the active site via hydrogen bonding.

Role of Asp-129. One of the most striking results from the present study is that Asp-129 in BPTP is critical to the overall binding of PLP. Even the conservative replacement of Asp-129 by a glutamic acid residue causes a dramatic decrease in the strength of binding of PLP, with the K_i increasing from 7.6 to 400 μM (Table 4). In the case of the hydrolysis of *p*NPP by wild-type BPTP, the dephosphorylation of the cysteinyl phosphate covalent intermediate is normally rate determining, and it is known that small, nucleophilic phosphate acceptors such as methanol increase the turnover rate of the enzyme with substrates such as *p*NPP (*11*). In the present case, however, partitioning experiments showed that the hydrolysis of PLP was unaffected by the presence of such small nucleophilic phosphate acceptors (Figure 5A). This indicated that the rate-determining step in the hydrolysis of PLP by WT-BPTP is changed to the phosphorylation step. This striking alteration in the kinetic mechanism suggested that the interaction of PLP with WT-BPTP must result in perturbation of one of the critical catalytic residues required in the phosphorylation step. Consistent with the results of mutagenesis studies and molecular mechanics modeling, this residue is almost certainly Asp-129, which is normally the proton donor to the leaving group during the phosphorylation step (*18*). It appears likely that the carboxylate group of Asp-129 interacts with the pyridinium nitrogen of the bound PLP. Such an interaction apparently affects the orientation and probably the pK_a of the Asp-129 residue and disrupts its proton donor

function. This conclusion is nicely consistent with the results seen for the D129E-BPTP-catalyzed hydrolysis of *p*NPP and PLP, where the rates of both slow hydrolysis reactions were enhanced by methanol (Figure 5B). Thus, the dephosphorylation step is still largely rate determining. This implies that the binding of PLP does not interfere with the proton donor function of Glu-129 and suggests that there is little or no direct interaction between the carboxyl group of Glu-129 and the pyridinium nitrogen of PLP. Consistent with this, D129E-BPTP binds PLP poorly. Such a conclusion is also consistent with fluorescence measurements (Table 5).

Energy minimization calculations yield results that are consistent with the critical role that Asp-129 appears to play in the PLP binding (Figure 6). The minimized structure with the lowest total energy showed that there are hydrogen bonds between the carboxyl group of Asp-129 and the proton on the pyridinium nitrogen of the bound PLP (Figure 7A). In contrast, hydrogen bond interactions involving the hydrogen on the pyridinium nitrogen of bound PLP and the carboxyl group of D129E-BPTP are quite different in the energy-minimized D129E-BPTP-PLP complex (Figure 7B). There is no hydrogen bond between the carboxyl group of Glu-129 and the hydrogen on the pyridinium nitrogen of bound PLP. Instead, the hydroxyl group of Tyr-132 forms hydrogen bonds with the hydrogen on the pyridinium nitrogen of bound PLP and the carboxyl group of Glu-129. The proton donor function of residue 129 is also disrupted. The pK_a value of Glu-129 is 6.30 (Z. Zhang, unpublished results). In the case of WT-BPTP, the pK_a value of Asp-129 is 5.30 (*42*). The relatively high value for Glu-129 may indicate the existence of a stabilizing hydrogen bond between the carboxylic acid form of Glu-129 and a nearby residue.

In most other protein−PLP complexes that have been studied, covalent interactions between the proteins and PLP are involved. In the present case, however, PLP strongly interacts with BPTP but the interactions are noncovalent. PLP can inhibit BPTP as strongly as vanadate ion, which is a commonly used inhibitor for many phosphatases and which has a broad inhibition spectrum. However, unlike the smaller vanadate ion, transition state analogue (*19*), the binding strength of PLP is contributed from every part of a complex molecule. Necessarily, multiple amino acid residues of the enzyme (but notably excluding Cys-17) contribute complementary sites to complete the binding interactions (Figure 8). The structural identifications made here, particularly the hydrogen bond interaction between the carboxylate group of Asp-129 and the pyridinium nitrogen, serve to clarify the mystery of the strong binding but poor catalysis involving PLP and the BPTP active site. The present picture also represents what should be extremely useful information in the design of specific inhibitors of the phosphatase. Although structural information is not yet available for the erythrocyte phosphatase studied by Fonda and colleagues, there may be some similarities with the low molecular weight PTPase studied here, beyond the fact that both enzymes have active site cysteine residues and that catalysis involves the formation of a covalent phosphoenzyme intermediate. The present structural examinations may help to model the active site of the pyridoxal phosphatase, and they should certainly be of benefit to the structure−function analyses of other PTPase families.

ACKNOWLEDGMENT

We thank Patrick Tishmack for NMR technical suggestions and helpful discussions, Christine Pokalsky for fluorescence technical suggestions, Dr. Etti Harms, Dr. Bonnie Evans, and Dr. June Davis for the site-directed mutagenesis, and Dr. Marie Zhang for helpful discussions.

REFERENCES

1. Hunter, T. (1995) *Cell 80*, 225−236.
2. Hunter, T. (1998) *Philos. Trans. R. Soc. London, Ser. B 353*, 583−605.
3. Fischer, E. H., Charbonneau, H., and Tonks, N. K. (1991) *Science 253*, 401−406.
4. Wo, Y.-Y. P., Zhou, M.-M., Stevis, P., Davis, J. P., Zhang, Z.-Y., and Van Etten, R. L. (1992) *Biochemistry 31*, 1712−1721.
5. Wo, Y.-Y. P., MacCormack, A., Shabanowitz, J., Hunt, D. S., Davis, J. P., Mitchell, G., and Van Etten, R. L. (1992) *J. Biol. Chem. 267*, 10856−10865.
6. Zhang, M., Stauffacher, C. V., and Van Etten, R. L. (1995) *Adv. Protein Phosphatases 9*, 1−23.
7. Lawrence, G. L., and Van Etten, R. L. (1981) *Arch. Biochem. Biophys. 206*, 122−131.
8. Waheed, A., Laidler, P. M., Wo, Y.-Y. P., and Van Etten, R. L. (1988) *Biochemistry 27*, 4265−4273.
9. Zhang, Z.-Y., and Van Etten, R. L. (1990) *Arch. Biochem. Biophys. 228*, 39−49.
10. Zhang, Z.-Y., and Van Etten, R. L. (1991) *Biochemistry 30*, 8954−8959.
11. Zhang, Z.-Y., and Van Etten, R. L. (1991) *J. Biol. Chem. 266*, 1516−1525.
12. Davis, J. P., Zhou, M.-M., and Van Etten, R. L. (1994) *J. Biol. Chem. 269*, 8734−8740.
13. Davis, J. P., Zhou, M.-M., and Van Etten, R. L. (1994) *Biochemistry 33*, 1278−1286.
14. Logan, T., Zhou, M.-M., Nettesheim, D. G., Meadows, R. P., and Van Etten, R. L. (1994) *Biochemistry 33*, 11087−11096.
15. Su, X.-D., Taddei, N., Stefani, M., Ramponi, G., and Nordlund, P. (1994) *Nature 370*, 575−578.
16. Zhang, M., Van Etten, R. L., and Stauffacher, C. V. (1994) *Biochemistry 33*, 11097−11105.
17. Zhang, M., Stauffacher, C. V., Lin, D., and Van Etten, R. L. (1998) *J. Biol. Chem. 273*, 21714−21720.
18. Zhang, Z., Harms, E., and Van Etten, R. L. (1994) *J. Biol. Chem. 269*, 25947−25950.
19. Zhang, M., Zhou, M., Van Etten, R. L., and Stauffacher, C. V. (1997) *Biochemistry 36*, 15−23.
20. John, R. A. (1995) *Biochim. Biophys. Acta 1248*, 81−96.
21. Cirri, P., Chiarugi, P., Camici, G., Manao, G., Pazzagli, L., Caselli, A., Barghini, I., Cappugi, G., Raugei, G., and Ramponi, G. (1993) *Biochim. Biophys. Acta 1161*, 216−222.
22. Fonda, M. L. (1992) *J. Biol. Chem. 267*, 15978−15983.
23. Gao, G.-J., and Fonda, M. L. (1994) *J. Biol. Chem. 269*, 8234−8239.
24. Gao, G.-J., and Fonda, M. L. (1994) *Arch. Biochem. Biophys. 313*, 166−172.
25. Gao, G.-J., and Fonda, M. L. (1994) *J. Biol. Chem. 269*, 7163−7168.
26. Burke, T. R., Jr., Ye, B., Yan, X., Wang, S., Jia, Z., Chen, L., Zhang, Z.-Y., and Barford, D. (1996) *Biochemistry 35*, 15989−15996.
27. Beers, S. A., Malloy, E. A., Wu, W., Wachter, M. P., Gunnia, U., Cavender, D., Harris, C., Davis, J., Brosius, R., Pellegrino-Gensey, J. L., and Siekierka, J. (1997) *Bioorg. Med. Chem. 5*, 2203−2211.
28. Beers, S. A., Schwender, C. F., Loughney, D. A., Malloy, E., Demarest, K., and Jordan, J. (1996) *Bioorg. Med. Chem. 4*, 1693−1701.
29. Chiarugi, P., Cirri, P., Marra, E., Raugei, G., Camici, G., Manao, G., and Ramponi, G. (1997) *Biochem. Biophys. Res. Commun. 238*, 676−682.

30. Sawyer, T. K., Stables, D. J., Liu, L., Tomasselli, A. G., Hui, J. O., O'Connell, K., Schostarez, H., Hester, J. B., Moon, J., Howe, W. J., Smith, C. W., Decamp, D. L., Craik, C. S., Dunn, B. M., Lowther, W. T., Harris, J., Poorman, R. A., Wlodawer, A., Jaskolski, M., and Heinrikson, R. L. (1992) *Int. J. Pept. Protein Res. 40*, 274−281.
31. Baykov, A. A., Eutushenko, O. A., and Avaeva, S. M. (1988) *Anal. Biochem. 171*, 266−270.
32. Dixon, M. (1953) *Biochem. J. 55*, 170−171.
33. Black, M. J., and Jones, M. (1983) *Anal. Biochem. 135*, 233−238.
34. Pokalsky, C., Wick, P., Harms, E., Lytle, F. E., and Van Etten, R. L. (1995) *J. Biol. Chem. 270*, 3809−3815.
35. Ward, L. D. (1985) *Methods Enzymol. 117*, 400−415.
36. Norris, A. W., Cheng, L., Giguere, V., Rosenberger, M., and Li, E. (1994) *Biochim. Biophys. Acta 1209*, 10−18.
37. Harris, C. M., Johnson, R. J., and Metzler, D. E. (1976) *Biochim. Biophys. Acta 421*, 181−194.
38. Metzler, D. E., and Snell, E. E. (1955) *J. Am. Chem. Soc. 77*, 2431−2437.
39. Hargrove, J. L., and Wichman, R. D. (1987) *J. Biol. Chem. 262*, 7351−7357.
40. Zhou, M. M., Davis, J. P., and Van Etten, R. L. (1993) *Biochemistry 32*, 8479−8486.
41. Submeier, J. L., Evelhoch, J. L., and Jonsson, N. (1980) *J. Magn. Reson. 40*, 377−390.
42. Evans, B., Tishmack, P. A., Pokalsky, C., Zhang, M., and Van Etten, R. L. (1996) *Biochemistry 35*, 13609−13617.
43. Bendall, M. R., Cartwright, I. L., Clark, P. I., Lowe, G., Nurse D. (1977) *Eur. J. Biochem. 79*, 201−209.
44. Bone, R., Cullis, P., and Wolfenden, R. (1983) *J. Am. Chem. Soc. 105*, 1339−1343.
45. Metzler, D. E., Harris, C. M., Johnson, R. J., Siano, D. B., and Thomson, J. A. (1973) *Biochemistry 12*, 5377−5392.

BI9823737